Title

Elementary Decomposition Mechanisms of Lithium Hexafluorophosphate in Battery Electrolytes and Interphases

Journal

ACS Energy Letters, 8(1)

ISSN

2380-8195

Authors

Spotte-Smith, Evan Walter Clark
Petrocelli, Thea Bee
Patel, Hetal D
et al.

Publication Date

2023-01-13

DOI

10.1021/acsenergylett.2c02351

ACS Energy LETTERS

http://pubs.acs.org/journal/aelccp

Elementary Decomposition Mechanisms of Lithium Hexafluorophosphate in Battery Electrolytes and Interphases

Evan Walter Clark Spotte-Smith,[#] Thea Bee Petrocelli,[#] Hetal D. Patel, Samuel M. Blau, and Kristin A. Persson*

Cite This: *ACS Energy Lett.* 2023, 8, 347−355

Read Online

ACCESS | Metrics & More | Article Recommendations | Supporting Information

ABSTRACT: Electrolyte decomposition constitutes an outstanding challenge to long-life Li-ion batteries (LIBs) as well as emergent energy storage technologies, contributing to protection via solid electrolyte interphase (SEI) formation and irreversible capacity loss over a battery's life. Major strides have been made to understand the breakdown of common LIB solvents; however, salt decomposition mechanisms remain elusive. In this work, we use density functional theory to explain the decomposition of lithium hexafluorophosphate ($LiPF_6$) salt under SEI formation conditions. Our results suggest that $LiPF_6$ forms POF_3 primarily through rapid chemical reactions with Li_2CO_3, while hydrolysis should be kinetically limited at moderate temperatures. We further identify selectivity in the proposed autocatalysis of POF_3, finding that POF_3 preferentially reacts with highly anionic oxygens. These results provide a means of interphase design in LIBs, indicating that $LiPF_6$ reactivity may be controlled by varying the abundance or distribution of inorganic carbonate species or by limiting the transport of PF_6^- through the SEI.

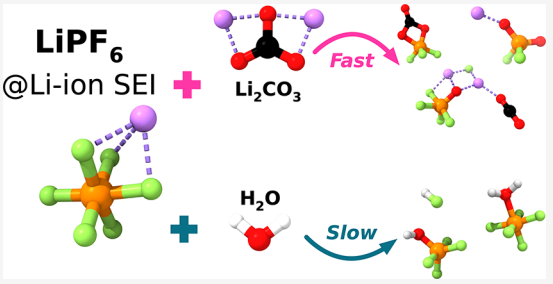

Lithium-ion batteries (LIBs) have in recent years become a cornerstone energy storage technology,[1] powering personal electronics and a growing number of electric vehicles. To continue this trend of electrification in transportation and other sectors, LIBs with higher energy density[2−5] and longer cycle and calendar life[6] are needed, motivating research into novel battery materials. Battery electrolytes, which are typically the limiting factor in terms of LIB potential window and irreversible capacity loss,[7−9] are an especially attractive target for research and development to expand the utility of LIBs.

In today's commercial LIBs, the most common electrolytes are comprised of lithium hexafluorophosphate ($LiPF_6$) dissolved in blends of cyclic carbonates, especially ethylene carbonate (EC), and linear carbonates such as ethyl methyl carbonate.[10−14] Carbonate/$LiPF_6$ electrolytes have many desirable properties, including weak ion association and high Li^+ conductivity,[15−17] but they are reactive at low potentials. When paired with graphite negative electrodes, carbonate/$LiPF_6$ electrolytes decompose to form a relatively stable passivation film known as the solid electrolyte interphase (SEI),[18−23] which prevents continual electrolyte degradation while allowing reversible charging and discharging. On the other hand, conventional electrolytes based on EC and $LiPF_6$ are essentially incompatible with high-energy density negative electrodes (e.g., Li metal,[24,25] Si[26,27]) and form unstable SEIs, resulting in comparatively poor cycle and calendar life.[28,29]

Due to the significance of the SEI in preserving battery capacity, SEI formation from carbonate/$LiPF_6$ electrolytes has been extensively studied for decades.[30−32] Such studies have sought to reveal the fundamental processes involved in the exemplar carbonate/$LiPF_6$ system and to identify opportunities for improvement through electrolyte engineering. An understanding of the decomposition of carbonate solvents, particularly EC, has been developed via a combination of experiment and theory. A wide range of decomposition products (including gases,[33,34] short-chain organic molecules, oligomers/polymers, and inorganic carbonates (e.g., Li_2CO_3) and oxides (e.g., Li_2O)[19]) have been experimentally characterized, and plausible elementary mechanisms for EC decomposition have been identified using density functional

Received: October 17, 2022
Accepted: November 21, 2022
Published: December 5, 2022

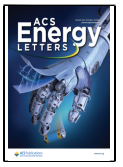

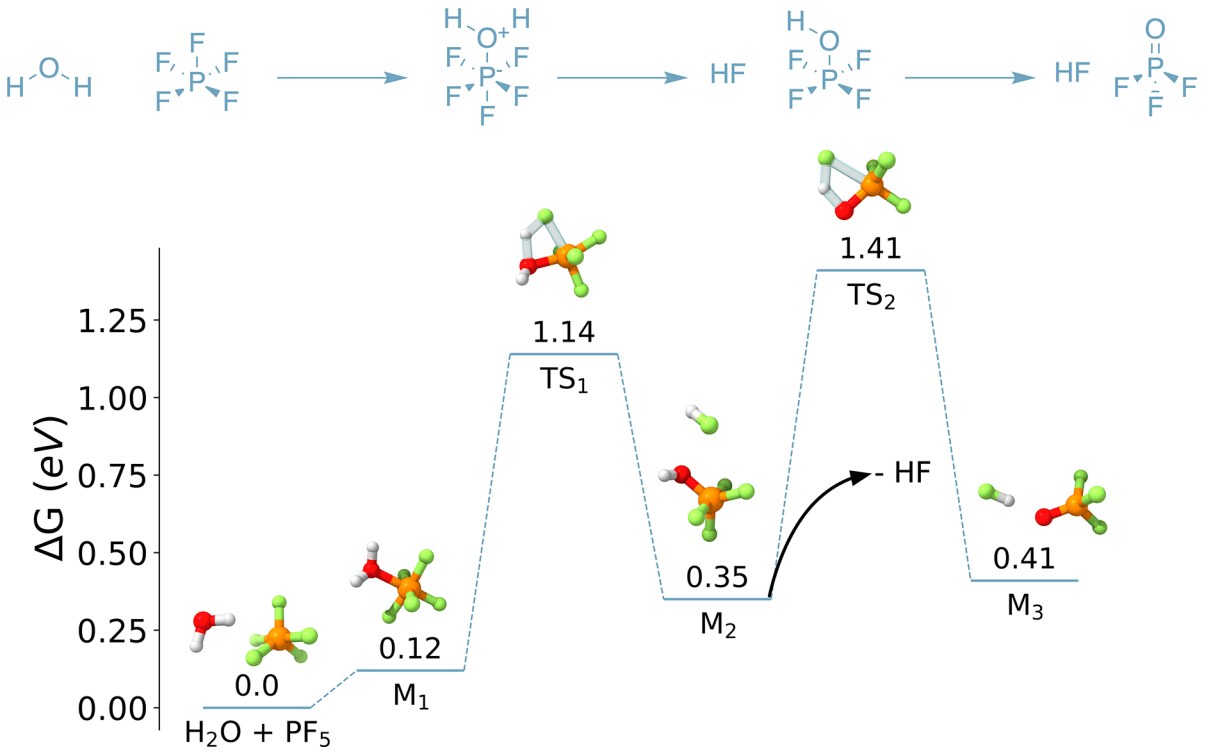

Figure 1. Hydrolysis of PF_5 to form POF_3 and 2HF. This mechanism is overall thermodynamically unfavorable and involves two reactions with high barriers ($\Delta G^{\ddagger}$ > 1.00 eV).

theory (DFT),[35−37] *ab initio* molecular dynamics (AIMD),[38−40] and chemical reaction network analysis.[41−44]

$$POF_3 + R_2CO_3 \rightarrow PF_2O_2R + RF + CO_2 \quad (1)$$

$$PF_2O_2R + PF_5 \rightarrow RF + 2POF_3 \quad (2)$$

In comparison, there are many open questions concerning the decomposition of $LiPF_6$. It is widely accepted that $LiPF_6$ reacts to form LiF, which precipitates and contributes to the SEI.[30,31,45,46] A range of other products, including POF_3,[47] difluorophosphoric acid (PF_2OOH),[48] and some organophosphorus compounds[49] have been identified by experimental spectroscopy. Moreover, $LiPF_6$ demonstrates thermal instability,[50,51] and it has long been suggested that an autocatalytic mechanism involving POF_3 (eqs 1 and 2) is responsible.[52] However, mechanistic explanations for $LiPF_6$ reactivity remain lacking. Most commonly, hydrolysis[7,45,46,51,53] is invoked to explain observed PF_6^- decomposition products (eqs 3 and 4 show an example mechanism). $LiPF_6$ has been shown to be unstable in the presence of water,[14] yet hydrolysis alone is insufficient to explain the significant role of $LiPF_6$ in SEI formation. The DFT study of Okamoto[54] suggests that PF_6^- hydrolysis should be extremely slow, in agreement with longstanding experimental evidence.[55] Moreover, LIB electrolytes used in laboratory studies are often rigorously dried, allowing ∼10 ppm of H_2O. Though exposure to high potentials on the positive electrode can both enable the formation of H_2O by reactions with EC[56] and accelerate PF_6^- hydrolysis,[57] this cannot explain LiF formation or further $LiPF_6$ decomposition during early SEI formation before high potentials have been reached or in batteries without high-voltage positive electrodes.

$$LiPF_6 \rightleftharpoons LiF(s) + PF_5 \quad (3)$$

$$PF_5 + H_2O \rightarrow POF_3 + 2HF \quad (4)$$

In this work, we explore the decomposition mechanisms of $LiPF_6$ using DFT at a high level of theory (see Supporting Information for details). We find that water is not necessary to explain the formation of LiF or POF_3 but rather that PF_5 can react rapidly with readily available Li_2CO_3 during early SEI formation. This mechanism is entirely chemical in nature; it does not depend on electrochemical reduction or oxidation of $LiPF_6$ and can occur at any depth of the SEI as long as the transport of PF_6^- to inorganic carbonate domains is feasible. Hence, the porosity, morphology, and transport properties of the SEI also become relevant factors. We then study POF_3 autocatalysis, using PF_2OOH and $LiPF_2O_2$ as model intermediates. Because POF_3 adds selectively to highly charged oxygens in oxyanions, $LiPF_2O_2$ is preferred over PF_2OOH in the absence of an oxidizing potential. Our calculations indicate that overall, the POF_3 autocatalytic cycle is limited by a slow intramolecular fluorine transfer step. These findings answer longstanding questions regarding the decomposition of $LiPF_6$ and suggest new routes for controlling salt reactivity during SEI formation.

We begin by considering the formation of PF_5, which is a key intermediate in essentially all $LiPF_6$ reaction routes considered in the literature and in this work. We find that the elimination of LiF from $LiPF_6$ to form PF_5 (eq 3) has no transition state but is endergonic, with ΔG = 1.04 eV. However, we note that the product in this reaction is a solution-phase molecule of LiF, whereas we expect that LiF will precipitate, forming solid deposits within the SEI. The elimination of LiF is more likely to occur when considering the possibility that LiF could be stabilized by precipitation. Okamoto[54] previously found that the deposition of solid LiF (LiF(solv) → LiF(solid)) has ΔG = −1.17 eV, which would

https://doi.org/10.1021/acsenergylett.2c02351
ACS Energy Lett. 2023, 8, 347−355

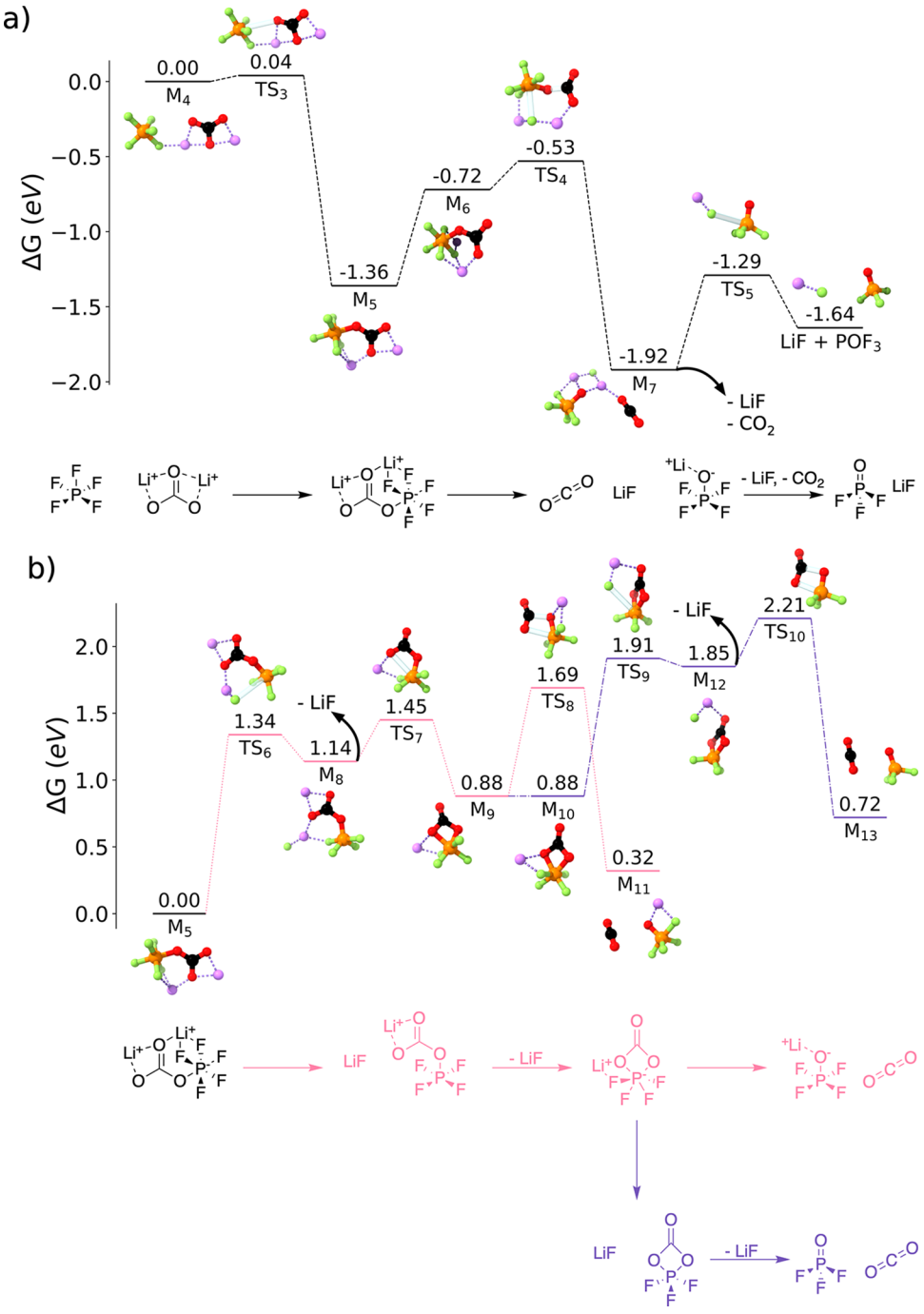

Figure 2. Energy diagrams for the formation of POF_3 from PF_5 and Li_2CO_3. (a) $LiPOF_4$ forms via by simultaneous elimination of LiF and CO_2 from a PF_5−Li_2CO_3 adduct. $LiPOF_4$ can then eliminate LiF to form POF_3. (b) Alternative, less favorable mechanisms in which LiF is eliminated from the adduct without simultaneously eliminating CO_2.

make eq 3 overall exergonic. More recently, Cao et al.[58] used DFT and AIMD to show that $LiPF_6$ decomposition by either chemical or electrochemical means is greatly accelerated in the presence of existing LiF. Here, we report the reaction energies and energy barriers of LiF elimination reactions like eq 3 without including the effect of a surface or LiF precipitation. However, we emphasize that these reactions, in general, should be more favorable than what is predicted based on calculations with molecular LiF in solution.

Even once PF_5 is formed, Figure 1 confirms that, at our chosen level of theory, the direct hydrolysis of PF_5 by H_2O is unfavorable. Each of the three hydrolysis steps (the addition of H_2O to PF_5 ($H_2O + PF_5 \rightarrow M_1$), the elimination of HF to form PF_4OH ($M_1 \rightarrow M_2$), and the elimination of another HF from PF_4OH to form POF_3 ($M_2 \rightarrow M_3$)) is predicted to be endergonic. Further, the last two steps both have energy barriers $\Delta G^{\ddagger} > 1.00$ eV, agreeing with the experimental observation that hydrolysis is slow at room temperature. Significant thermal activation beyond temperatures reached in normal LIB cycling conditions would be required to enable $LiPF_6$ hydrolysis.

An alternative mechanism involves the reaction of PF_5 with Li_2CO_3 (Figure 2). Reactions between $LiPF_6$ and inorganic carbonates have been proposed in the past[59,60] on the basis of

https://doi.org/10.1021/acsenergylett.2c02351
ACS Energy Lett. 2023, 8, 347−355

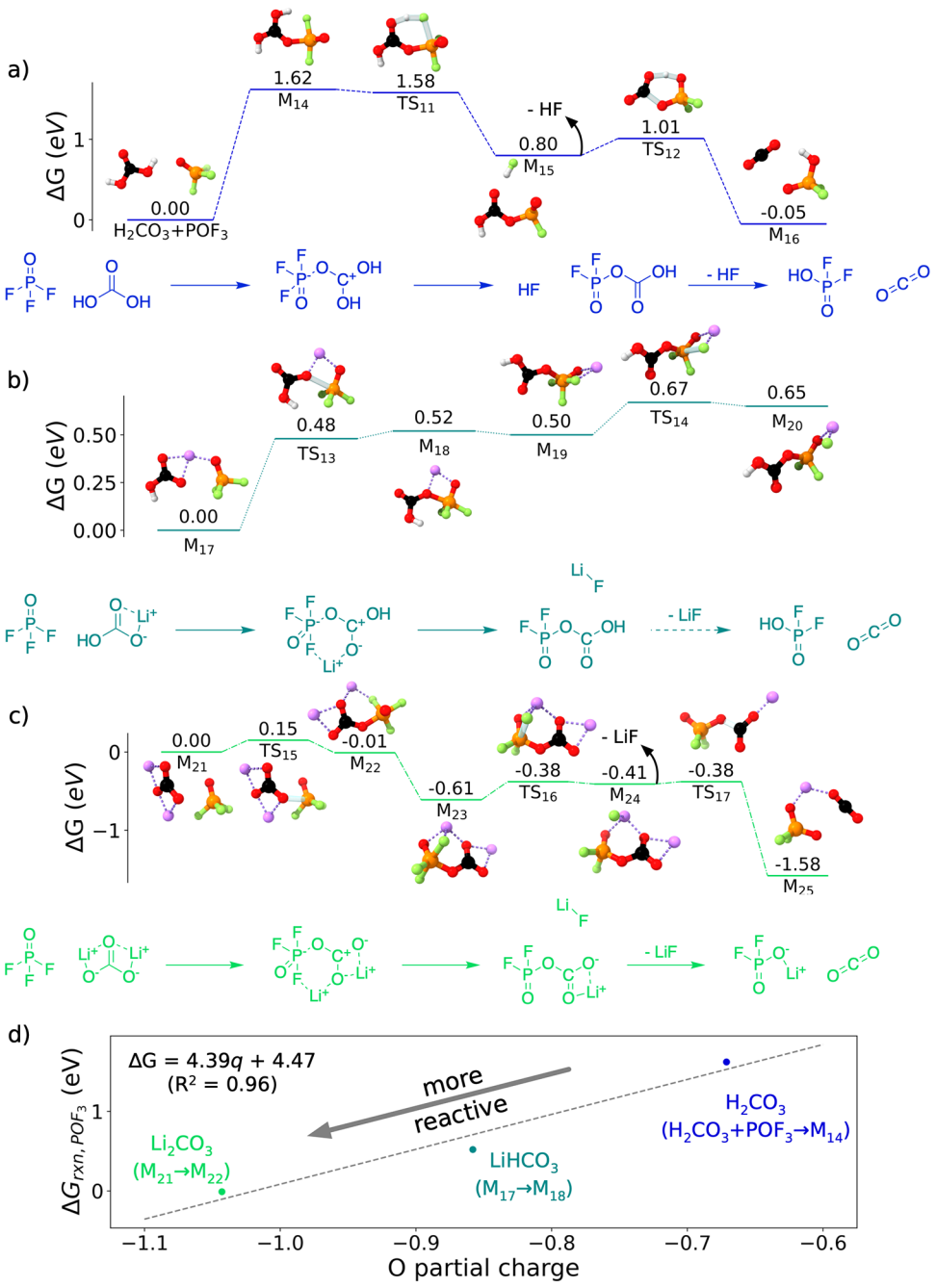

Figure 3. Reactions between POF_3 and simple inorganic carbonates (a) H_2CO_3, (b) $LiHCO_3$, and (c) Li_2CO_3 to form CO_2 and either PF_2OOH or $LiPF_2O_2$. A trend between the partial charge of the reacting oxygen(s) and the reaction energies with POF_3 for each carbonate considered is shown in (d). A linear fit, $\Delta G = 4.39q + 4.47$, where q is the most negative oxygen partial charge, shows strong correlation ($R^2 = 0.96$) among the three carbonates.

the observed evolution of CO_2 and POF_3 upon mixing of $LiPF_6$ and Li_2CO_3, but this route has largely been neglected in favor of hydrolytic mechanisms. Moreover, no elementary mechanism for the reaction between $LiPF_6$-like species and Li_2CO_3 has been reported.

We find that PF_5 reacts vigorously with Li_2CO_3. An initial addition step between the two reactants ($M_4 \rightarrow M_5$) has a low barrier of $\Delta G^{\ddagger} = 0.04$ eV. Following reorganization of Li^+ ($M_5 \rightarrow M_6$), the adduct (M_6) then dissociates in a single concerted reaction, yielding LiF, CO_2, and $LiPOF_4$ with $\Delta G^{\ddagger} = 0.19$ eV. Finally, to form POF_3, $LiPOF_4$ eliminates an additional molecule of LiF ($M_7 \rightarrow$ LiF + POF_3), with $\Delta G^{\ddagger} = 0.63$ eV, $\Delta G = 0.28$ eV. We again note that we expect both ΔG and $\Delta G^{\ddagger}$ for LiF elimination reactions to be lowered if precipitation of LiF on a surface is allowed. Even without any corrections for the instability of molecular LiF produced in $M_6 \rightarrow M_7$ and $M_7 \rightarrow$ LiF + POF_3, this mechanism represents one of the most kinetically favorable elementary mechanisms for PF_5 decomposition yet reported.

If it does not dissociate completely, the adduct M_5 may instead eliminate LiF ($M_5 \rightarrow M_8$), though this reaction suffers from a high predicted barrier of $\Delta G^{\ddagger} = 1.34$ eV. After LiF elimination, an additional oxygen from the carbonate group binds to phosphorus to form a ring complex M_9. By eliminating

https://doi.org/10.1021/acsenergylett.2c02351
ACS Energy Lett. 2023, 8, 347−355

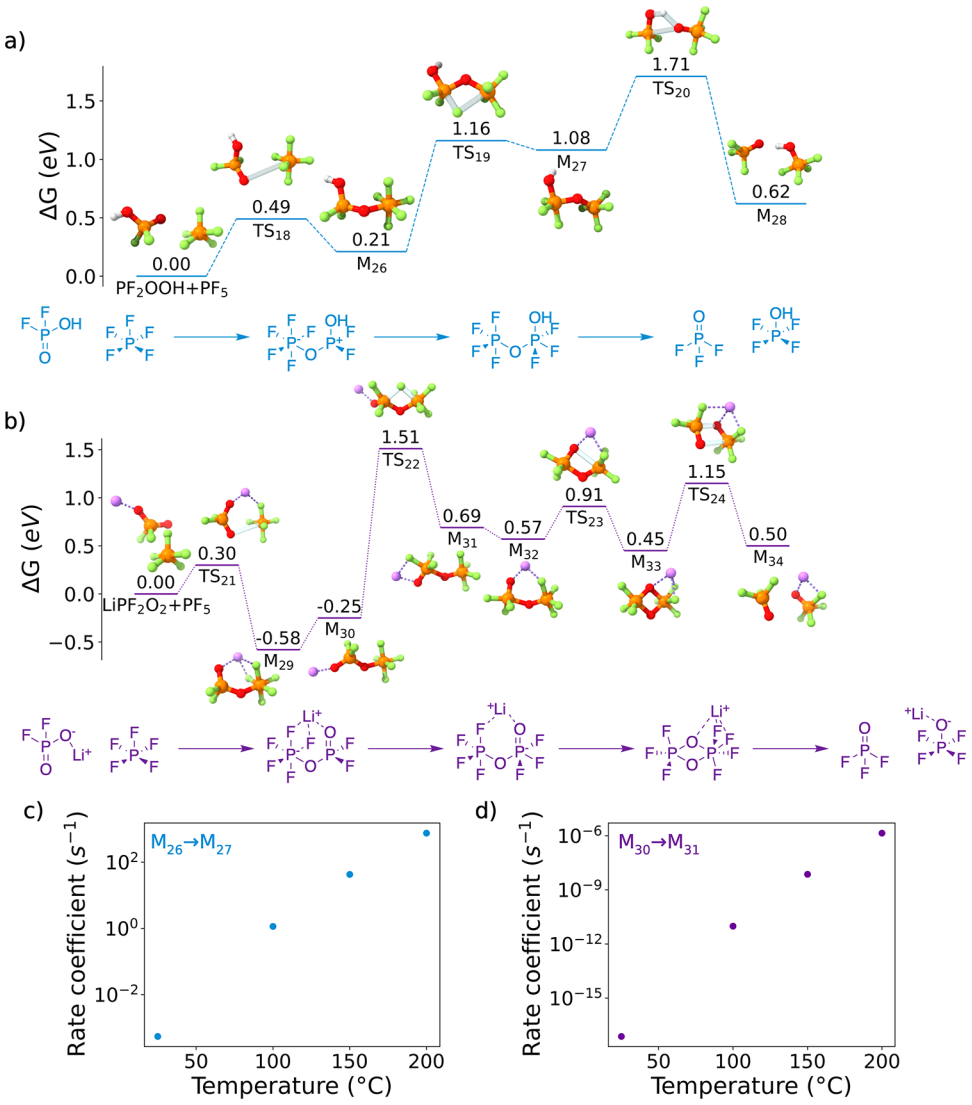

Figure 4. Possible routes for the re-formation of POF_3 from PF_2OOH (a) and $LiPF_2O_2$ (b). Both mechanisms are kinetically limited due to an extremely unfavorable intramolecular fluorine transfer step ($M_{26} \rightarrow M_{27}$, $M_{30} \rightarrow M_{31}$), which makes POF_3 autocatalysis unlikely at modest temperatures. Rate coefficients for the fluorine transfer step are provided in (c) for the PF_2OOH pathway and in (d) for the $LiPF_2O_2$ pathway.

CO_2, either immediately ($M_9 \rightarrow M_{11}$, $\Delta G^{\ddagger}$ = 0.81 eV) or following the elimination of another LiF ($M_{12} \rightarrow M_{13}$, $\Delta G^{\ddagger}$ = 0.36 eV), this ring complex also forms $LiPOF_4$ (M_{11}) or POF_3 (M_{13}).

The proposed mechanisms shown in Figure 2 rely only on Li_2CO_3, which should be abundant at the negative electrode, especially during early SEI formation.[21,31,38,60−62] The reaction of PF_5 and Li_2CO_3 is also entirely chemical in nature; none of the reactions in Figure 2 depend on electrochemical oxidation or reduction. As a result, the decomposition should not depend explicitly on applied potential, the proximity to the anode surface, or the availability of electrons. We therefore predict that the decomposition of PF_5 can occur anywhere in the SEI, so long as inorganic carbonates like Li_2CO_3 are present. This being said, because Li_2CO_3 is formed in the SEI as a result of electrochemical reduction of EC,[38,44] the overall rate of POF_3 formation via the reaction of PF_5 with Li_2CO_3 will implicitly have a potential dependence.

While our focus in this work is on $LiPF_6$ decomposition during SEI formation, it is worth noting that Li_2CO_3 is an impurity formed during the synthesis of common transition metal oxide positive electrodes.[59] Accordingly, the mechanisms described in Figure 2 could occur at the positive electrode as well as at the negative electrode or the SEI.

Figure 2 indicates that POF_3 emerges rapidly by reaction with Li_2CO_3 during SEI formation. This hints that the proposed autocatalytic mechanisms for POF_3 (re-)formation (eqs 1 and 2), which rely on POF_3 and carbonate species, are chemically plausible.

To confirm the mechanism of POF_3 autocatalysis at elevated temperature, we first consider the formation of PF_2O_2R species (Figure 3). Specifically, we explore the formation of PF_2OOH from H_2CO_3 (Figure 3a) and $LiHCO_3$ (Figure 3b) and the formation of $LiPF_2O_2$ by Li_2CO_3 (Figure 3c). In addition to their relevance for POF_3 formation and $LiPF_6$ decomposition, PF_2O_2R species and in particular PF_2OOH have been blamed as major contributors to the decomposition of SEI species and the loss of battery capacity.[63,64] Jayawardana et al. have argued that PF_2OOH should form at the positive electrode as a result of PF_6^- oxidation.[63] If PF_2OOH and related species could

https://doi.org/10.1021/acsenergylett.2c02351
ACS Energy Lett. 2023, 8, 347−355

form at the negative electrode without high potentials, it could have significant implications for the stability of the SEI.

Figure 3a shows a mechanism for a chemical reaction between H_2CO_3 and POF_3. The initial addition reaction between POF_3 and H_2CO_3 ($H_2CO_3 + POF_3 \rightarrow M_{14}$) is thermodynamically unfavorable (ΔG = 1.62 eV). Subsequent reactions to form HF, CO_2, and PF_2OOH do not face significant barriers and should occur rapidly. The reaction between POF_3 and $LiHCO_3$ (Figure 3b) follows a similar mechanism. The addition step ($M_{17} \rightarrow M_{18}$) is also endergonic ($\Delta G^{\ddagger}$ = 0.48 eV, ΔG = 0.52 eV), though we suggest that it could be accessed at moderate temperatures. Addition by $LiHCO_3$ is followed by the elimination of LiF ($M_{19} \rightarrow M_{20}$), which is analogous to the elimination of HF in Figure 3a ($M_{14} \rightarrow M_{15}$). Following the complete removal of LiF, M_{20} can undergo the same concerted proton transfer and CO_2 elimination shown in Figure 3a ($M_{15} \rightarrow M_{16}$).

In contrast, POF_3 adds easily to Li_2CO_3 (Figure 3c, $M_{21} \rightarrow M_{22}$), with $\Delta G^{\ddagger}$ = 0.15 eV and ΔG = −0.01 eV. We explain the difference in the thermodynamics of the reactions between POF_3 and H_2CO_3, $LiHCO_3$, and Li_2CO_3 by considering atomic partial charges (Figure 3d). POF_3 is reactive toward the highly anionic oxygens in Li_2CO_3 but not toward the less charged oxygens in $LiHCO_3$ and H_2CO_3. The difference in behavior can also be rationalized in terms of acid−base chemistry. POF_3 and PF_5 (both Lewis acids) prefer to react with CO_3^{2-} (a Lewis base) over HCO_3^- (depending on context, either a weak acid or a weak base) and H_2CO_3 (an acid). We find similar trends for the reaction between PF_5 and inorganic carbonates (Supporting Information Figure S1). Moreover, we suggest (Supporting Information Figure S2) that the reactivity of phosphorus fluorides with anionic oxygens and Lewis bases is at least somewhat general and is not specific to Li_2CO_3. Though PF_2OOH formation via $LiHCO_3$ is possible, the difficulty of addition with protonated carbonates suggests that, barring electrochemical processes, $LiPF_2O_2$ should be more abundant at the negative electrode than PF_2OOH. Nonetheless, the prediction that PF_2OOH and $LiPF_2O_2$ can form at or near the SEI without the need for cross-talk from the positive electrode motivates further efforts to understand the interactions between these species and other SEI components.

Mechanisms for the re-formation of POF_3, completing the autocatalytic cycle in eq 2, are shown in Figure 4. Following a similar trend to that shown in Figure 3d, the attack of PF_5 by the acidic PF_2OOH (Figure 4a, $PF_2OOH + PF_5 \rightarrow M_{26}$) is thermodynamically unfavorable, while $LiPF_2O_2$ can favorably add to PF_5 (Figure 4b, $LiPF_2O_2 + PF_5 \rightarrow M_{29}$). After the initial addition, an intramolecular fluorine transfer is required; for both PF_2O_2R species considered, this step is thermodynamically unfavorable and suffers from a high barrier ($M_{26} \rightarrow M_{27}$, $\Delta G^{\ddagger}$ = 0.95 eV; $M_{30} \rightarrow M_{31}$, $\Delta G^{\ddagger}$ = 1.76 eV). While both intramolecular fluorine transfer reactions are kinetically limited at room temperature (Figure 4c,d), the reaction without Li^+ can occur at elevated temperature (especially T > 150 °C). After fluorine transfer, the two mechanisms in Figure 4a,b diverge. In Figure 4a, a concerted proton transfer and elimination step occurs ($M_{27} \rightarrow M_{28}$), yielding POF_3 and PF_4OH. PF_4OH can subsequently eliminate HF to form POF_3, as shown in Figure 1. In Figure 4b, a four-member O−P−O−P ring is formed ($M_{32} \rightarrow M_{33}$) and POF_3 is eliminated ($M_{33} \rightarrow M_{34}$), leaving $LiPOF_4$ which could then form LiF and POF_3 as previously discussed.

Our mechanism confirms the previously reported autocatalytic formation of POF_3. We find, in agreement with earlier experimental studies,[50,52] that this cycle requires significant thermal activation ($T \sim$ 150 °C). This is primarily due to a sluggish intramolecular fluorine transfer and, specifically for the mechanism requiring PF_2OOH as an intermediate, the high barrier for HF elimination to re-form POF_3. While we have found a mechanism for POF_3 autocatalysis that does not require any water, the significantly lower barrier for the pathway involving PF_2OOH indicates that $LiPF_6$ thermal decomposition could be initiated and accelerated by $LiPF_6$ hydrolysis,[47] which is accessible at elevated temperature.

To conclude, $LiPF_6$ is an exceptional salt that is likely to play a major role in the LIB market for years to come. While some decomposition of $LiPF_6$ is desirable to form a functional SEI, continued breakdown can severely limit the life of LiBs. In this work, we identified a novel and facile elementary decomposition mechanism of $LiPF_6$ using first-principles DFT simulations. Our results imply that under normal battery cycling conditions, the major decomposition mechanism of $LiPF_6$ does not depend on water or on electrochemical salt reduction. Rather, $LiPF_6$ forms the expected products LiF, POF_3, $LiPF_2O_2$, and potentially PF_2OOH via entirely chemical reactions with inorganic carbonates (especially Li_2CO_3). These reactions can likely occur in the solution phase or in nanocrystalline or amorphous regions of the SEI (see Supporting Information Table S1). PF_5 and POF_3 show a strong affinity to react with highly anionic oxygens and Lewis bases, suggesting that efforts to control the reactivity of $LiPF_6$ should focus on limiting the exposure of PF_5 to oxyanion and other basic species, including and especially inorganic carbonates like Li_2CO_3, in the SEI as well as on the surface of positive electrodes. This consideration may include morphological control, such as reducing porosity and/or abundance of inorganic species in the outer regions of the SEI.

In the future, theoretical studies should be combined with experimental spectroscopy to validate the mechanisms reported here. It should be possible to compare rate laws obtained by experiment (via, for example, time-resolved spectroscopy with varying amounts of inorganic carbonates and $LiPF_6$) and theory (via kinetic simulations, for example, kinetic Monte Carlo). More challenging but no less worthwhile would be to confirm if the decomposition of $LiPF_6$ in a battery is primarily chemical or electrochemical in nature. This could be accomplished by tracking the rate of decomposition of $LiPF_6$ in the presence of inorganic carbonate species in a reductively stable solvent under varying applied potentials. While we have focused here primarily on $LiPF_6$ decomposition in EC-based electrolytes, we suspect that $LiPF_6$ could chemically react in a range of solvents via mechanisms similar to what we have described, provided that those solvents reduce and decompose to form oxyanions with highly charged reactive oxygens or sufficiently strong Lewis bases. The extent of $LiPF_6$ decomposition will depend on the availability of these basic and oxyanion species. Additional investigations into solvent degradation and SEI formation in EC-free (and especially carbonate-free) electrolytes should be conducted to assess if the mechanism that we have described here is general or specific to carbonate-based solvents. Detailed study of the elementary reaction mechanisms between $LiPF_6$ decomposition products (especially PF_2O_2R species) and other SEI species (e.g., organic carbonates), as well as the formation

https://doi.org/10.1021/acsenergylett.2c02351
ACS Energy Lett. 2023, 8, 347−355

mechanisms of organophosphorus compounds and phosphate polymers in the SEI, should also be conducted.

■ ASSOCIATED CONTENT

Supporting Information

The Supporting Information is available free of charge at https://pubs.acs.org/doi/10.1021/acsenergylett.2c02351.

Data availability statement, computational methods, and discussion of additional reaction mechanisms for $LiPF_6$ decomposition (PDF)

■ AUTHOR INFORMATION

Corresponding Author

Kristin A. Persson − *Department of Materials Science and Engineering, University of California, Berkeley, Berkeley, California 94720, United States; Molecular Foundry, Lawrence Berkeley National Laboratory, Berkeley, California 94720, United States;* orcid.org/0000-0003-2495-5509; Email: kapersson@lbl.gov

Authors

Evan Walter Clark Spotte-Smith − *Materials Science Division, Lawrence Berkeley National Laboratory, Berkeley, California 94720, United States; Department of Materials Science and Engineering, University of California, Berkeley, Berkeley, California 94720, United States;* orcid.org/0000-0003-1554-197X

Thea Bee Petrocelli − *Materials Science Division, Lawrence Berkeley National Laboratory, Berkeley, California 94720, United States; Department of Materials Science and Engineering, University of California, Berkeley, Berkeley, California 94720, United States; Cabrillo College, Aptos, California 95003, United States*

Hetal D. Patel − *Materials Science Division, Lawrence Berkeley National Laboratory, Berkeley, California 94720, United States; Department of Materials Science and Engineering, University of California, Berkeley, Berkeley, California 94720, United States*

Samuel M. Blau − *Energy Storage and Distributed Resources, Lawrence Berkeley National Laboratory, Berkeley, California 94720, United States;* orcid.org/0000-0003-3132-3032

Complete contact information is available at: https://pubs.acs.org/10.1021/acsenergylett.2c02351

Author Contributions

#E.W.C.S.-S. and T.B.P. contributed equally to this work. Conceptualization: E.W.C.S.-S., K.A.P. Formal analysis: E.W.C.S.-S., T.B.P., H.D.P. Funding acquisition: E.W.C.S.-S., H.D.P., S.M.B., K.A.P. Investigation: E.W.C.S.-S., T.B.P., H.D.P. Resources: K.A.P. Supervision: E.W.C.S.-S., K.A.P. Visualization: E.W.C.S.-S. Writing of original draft: E.W.C.S.-S., T.B.P. Review and editing of manuscript: all authors.

Notes

The authors declare no competing financial interest.

■ ACKNOWLEDGMENTS

This work is intellectually led by the Silicon Consortium Project directed by Brian Cunningham under the Assistant Secretary for Energy Efficiency and Renewable Energy, Office of Vehicle Technologies of the U.S. Department of Energy, Contract DE-AC02-05CH11231 with additional support from the Joint Center for Energy Storage Research, an Energy Innovation Hub funded by the U.S. Department of Energy, Office of Science, Basic Energy Sciences. E.W.C.S.-S. is supported by the Kavli Energy Nanoscience Institute Philomathia Graduate Student Fellowship. H.D.P. is supported by the United States Department of Defense National Defense Science and Engineering Graduate Fellowship. S.M.B. is supoported by the Laboratory Directed Research and Development Program of Lawrence Berkeley National Laboratory under U.S. Department of Energy Contract DE-AC02-05CH11231. T.B.P. conducted this work as part of the Community College Internship program under the U.S. Department of Energy, Office of Science, Office of Workforce Development for Teachers and Scientists. Access to and assistance using the Schrödinger Suite of software tools, including Jaguar and AutoTS, were generously provided by Schrödinger, Inc. Data for this study were produced using computational resources provided by the Eagle and Swift high-performance computing (HPC) systems at the National Renewable Energy Laboratory and the Lawrencium HPC cluster at Lawrence Berkeley National Laboratory.

■ REFERENCES

(1) Li, M.; Lu, J.; Chen, Z.; Amine, K. 30 Years of Lithium-Ion Batteries. *Adv. Mater.* **2018**, *30*, 1800561.

(2) Evers, S.; Nazar, L. F. New Approaches for High Energy Density Lithium−Sulfur Battery Cathodes. *Acc. Chem. Res.* **2013**, *46*, 1135−1143.

(3) Cheng, X.-B.; Zhang, R.; Zhao, C.-Z.; Zhang, Q. Toward Safe Lithium Metal Anode in Rechargeable Batteries: A Review. *Chem. Rev.* **2017**, *117*, 10403−10473.

(4) Liu, B.; Zhang, J.-G.; Xu, W. Advancing Lithium Metal Batteries. *Joule* **2018**, *2*, 833−845.

(5) Voronina, N.; Sun, Y.-K.; Myung, S.-T. Co-Free Layered Cathode Materials for High Energy Density Lithium-Ion Batteries. *ACS Energy Lett.* **2020**, *5*, 1814−1824.

(6) Kalaga, K.; Rodrigues, M.-T. F.; Trask, S. E.; Shkrob, I. A.; Abraham, D. P. Calendar-life versus cycle-life aging of lithium-ion cells with silicon-graphite composite electrodes. *Electrochim. Acta* **2018**, *280*, 221−228.

(7) Aurbach, D.; Talyosef, Y.; Markovsky, B.; Markevich, E.; Zinigrad, E.; Asraf, L.; Gnanaraj, J. S.; Kim, H.-J. Design of electrolyte solutions for Li and Li-ion batteries: a review. *Electrochim. Acta* **2004**, *50*, 247−254.

(8) Logan, E. R.; Dahn, J. R. Electrolyte Design for Fast-Charging Li-Ion Batteries. *Trends Chem.* **2020**, *2*, 354−366.

(9) Li, Q.; Liu, G.; Cheng, H.; Sun, Q.; Zhang, J.; Ming, J. Low-Temperature Electrolyte Design for Lithium-Ion Batteries: Prospect and Challenges. *Chem.—Eur. J.* **2021**, *27*, 15842−15865.

(10) Blomgren, G. E. Electrolytes for advanced batteries. *J. Power Sources* **1999**, *81*−*82*, 112−118.

(11) Zhang, S. S.; Jow, T. R.; Amine, K.; Henriksen, G. L. LiPF6−EC−EMC electrolyte for Li-ion battery. *J. Power Sources* **2002**, *107*, 18−23.

(12) Xu, K. Nonaqueous Liquid Electrolytes for Lithium-Based Rechargeable Batteries. *Chem. Rev.* **2004**, *104*, 4303−4418.

(13) Wagner, R.; Preschitschek, N.; Passerini, S.; Leker, J.; Winter, M. Current research trends and prospects among the various materials and designs used in lithium-based batteries. *J. Appl. Electrochem.* **2013**, *43*, 481−496.

(14) Stich, M.; Göttlinger, M.; Kurniawan, M.; Schmidt, U.; Bund, A. Hydrolysis of LiPF6 in Carbonate-Based Electrolytes for Lithium-Ion Batteries and in Aqueous Media. *J. Phys. Chem. C* **2018**, *122*, 8836−8842.

(15) Seo, D. M.; Reininger, S.; Kutcher, M.; Redmond, K.; Euler, W. B.; Lucht, B. L. Role of Mixed Solvation and Ion Pairing in the Solution Structure of Lithium Ion Battery Electrolytes. *J. Phys. Chem. C* **2015**, *119*, 14038−14046.

(16) Hou, T.; Yang, G.; Rajput, N. N.; Self, J.; Park, S.-W.; Nanda, J.; Persson, K. A. The influence of FEC on the solvation structure and reduction reaction of LiPF6/EC electrolytes and its implication for solid electrolyte interphase formation. *Nano Energy* **2019**, *64*, 103881.
(17) Hou, T.; Fong, K. D.; Wang, J.; Persson, K. A. The solvation structure, transport properties and reduction behavior of carbonate-based electrolytes of lithium-ion batteries. *Chem. Sci.* **2021**, *12*, 14740−14751.
(18) Aurbach, D.; Markovsky, B.; Shechter, A.; Ein-Eli, Y.; Cohen, H. A Comparative Study of Synthetic Graphite and Li Electrodes in Electrolyte Solutions Based on Ethylene Carbonate-Dimethyl Carbonate Mixtures. *J. Electrochem. Soc.* **1996**, *143*, 3809.
(19) Verma, P.; Maire, P.; Novák, P. A review of the features and analyses of the solid electrolyte interphase in Li-ion batteries. *Electrochim. Acta* **2010**, *55*, 6332−6341.
(20) Agubra, V.; Fergus, J. Lithium Ion Battery Anode Aging Mechanisms. *Materials* **2013**, *6*, 1310−1325.
(21) Nie, M.; Chalasani, D.; Abraham, D. P.; Chen, Y.; Bose, A.; Lucht, B. L. Lithium Ion Battery Graphite Solid Electrolyte Interphase Revealed by Microscopy and Spectroscopy. *J. Phys. Chem. C* **2013**, *117*, 1257−1267.
(22) Agubra, V. A.; Fergus, J. W. The formation and stability of the solid electrolyte interface on the graphite anode. *J. Power Sources* **2014**, *268*, 153−162.
(23) Heiskanen, S. K.; Kim, J.; Lucht, B. L. Generation and Evolution of the Solid Electrolyte Interphase of Lithium-Ion Batteries. *Joule* **2019**, *3*, 2322−2333.
(24) Cheng, X.-B.; Zhang, R.; Zhao, C.-Z.; Wei, F.; Zhang, J.-G.; Zhang, Q. A Review of Solid Electrolyte Interphases on Lithium Metal Anode. *Adv. Sci.* **2016**, *3*, 1500213.
(25) Xue, W.; Shi, Z.; Huang, M.; Feng, S.; Wang, C.; Wang, F.; Lopez, J.; Qiao, B.; Xu, G.; Zhang, W.; Dong, Y.; Gao, R.; Shao-Horn, Y.; Johnson, J. A.; Li, J. FSI-inspired solvent and "full fluorosulfonyl" electrolyte for 4 V class lithium-metal batteries. *Energy Environ. Sci.* **2020**, *13*, 212−220.
(26) Nie, M.; Abraham, D. P.; Chen, Y.; Bose, A.; Lucht, B. L. Silicon Solid Electrolyte Interphase (SEI) of Lithium Ion Battery Characterized by Microscopy and Spectroscopy. *J. Phys. Chem. C* **2013**, *117*, 13403−13412.
(27) Philippe, B.; Dedryvère, R.; Gorgoi, M.; Rensmo, H.; Gonbeau, D.; Edström, K. Improved Performances of Nanosilicon Electrodes Using the Salt LiFSI: A Photoelectron Spectroscopy Study. *J. Am. Chem. Soc.* **2013**, *135*, 9829−9842.
(28) McBrayer, J. D.; et al. Calendar aging of silicon-containing batteries. *Nat. Energy* **2021**, *6*, 866−872.
(29) Boyle, D. T.; Huang, W.; Wang, H.; Li, Y.; Chen, H.; Yu, Z.; Zhang, W.; Bao, Z.; Cui, Y. Corrosion of lithium metal anodes during calendar ageing and its microscopic origins. *Nat. Energy* **2021**, *6*, 487−494.
(30) Aurbach, D.; Ein-Eli, Y.; Markovsky, B.; Zaban, A.; Luski, S.; Carmeli, Y.; Yamin, H. The Study of Electrolyte Solutions Based on Ethylene and Diethyl Carbonates for Rechargeable Li Batteries: II. Graphite Electrodes. *J. Electrochem. Soc.* **1995**, *142*, 2882.
(31) Aurbach, D.; Zaban, A.; Schechter, A.; Ein-Eli, Y.; Zinigrad, E.; Markovsky, B. The Study of Electrolyte Solutions Based on Ethylene and Diethyl Carbonates for Rechargeable Li Batteries: I. Li Metal Anodes. *J. Electrochem. Soc.* **1995**, *142*, 2873.
(32) Winter, M. The Solid Electrolyte Interphase − The Most Important and the Least Understood Solid Electrolyte in Rechargeable Li Batteries. *Z. Phys. Chem.* **2009**, *223*, 1395−1406.
(33) Rowden, B.; Garcia-Araez, N. A review of gas evolution in lithium ion batteries. *Energy Rep.* **2020**, *6*, 10−18.
(34) Zhao, H.; Wang, J.; Shao, H.; Xu, K.; Deng, Y. Gas Generation Mechanism in Li-Metal Batteries. *Energy Environ. Mater.* **2022**, *5*, 327−336.
(35) Ma, Y.; Balbuena, P. B. DFT Study of Reduction Mechanisms of Ethylene Carbonate and Fluoroethylene Carbonate on Li +-Adsorbed Si Clusters. *J. Electrochem. Soc.* **2014**, *161*, No. E3097.
(36) Gibson, L. D.; Pfaendtner, J. Solvent oligomerization pathways facilitated by electrolyte additives during solid-electrolyte interphase formation. *Phys. Chem. Chem. Phys.* **2020**, *22*, 21494−21503.
(37) Kuai, D.; Balbuena, P. B. Solvent Degradation and Polymerization in the Li-Metal Battery: Organic-Phase Formation in Solid-Electrolyte Interphases. *ACS Appl. Mater. Interfaces* **2022**, *14*, 2817−2824.
(38) Leung, K.; Budzien, J. L. Ab initio molecular dynamics simulations of the initial stages of solid−electrolyte interphase formation on lithium ion battery graphitic anodes. *Phys. Chem. Chem. Phys.* **2010**, *12*, 6583−6586.
(39) Soto, F. A.; Ma, Y.; Martinez de la Hoz, J. M.; Seminario, J. M.; Balbuena, P. B. Formation and Growth Mechanisms of Solid-Electrolyte Interphase Layers in Rechargeable Batteries. *Chem. Mater.* **2015**, *27*, 7990−8000.
(40) Young, J.; Kulick, P. M.; Juran, T. R.; Smeu, M. Comparative Study of Ethylene Carbonate-Based Electrolyte Decomposition at Li, Ca, and Al Anode Interfaces. *ACS Appl. Energy Mater.* **2019**, *2*, 1676−1684.
(41) Blau, S. M.; Patel, H. D.; Spotte-Smith, E. W. C.; Xie, X.; Dwaraknath, S.; Persson, K. A. A chemically consistent graph architecture for massive reaction networks applied to solid-electrolyte interphase formation. *Chem. Sci.* **2021**, *12*, 4931−4939.
(42) Xie, X.; Clark Spotte-Smith, E. W.; Wen, M.; Patel, H. D.; Blau, S. M.; Persson, K. A. Data-Driven Prediction of Formation Mechanisms of Lithium Ethylene Monocarbonate with an Automated Reaction Network. *J. Am. Chem. Soc.* **2021**, *143*, 13245−13258.
(43) Barter, D.; Spotte-Smith, E. W. C.; Redkar, N. S.; Khanwale, A.; Dwaraknath, S.; Persson, K. A.; Blau, S. M. Predictive stochastic analysis of massive filter-based electrochemical reaction networks. *ChemRxiv* **2022**, DOI: 10.26434/chemrxiv-2021-c2gp3-v3.
(44) Spotte-Smith, E. W. C.; Kam, R. L.; Barter, D.; Xie, X.; Hou, T.; Dwaraknath, S.; Blau, S. M.; Persson, K. A. Toward a Mechanistic Model of Solid−Electrolyte Interphase Formation and Evolution in Lithium-Ion Batteries. *ACS Energy Lett.* **2022**, *7*, 1446−1453.
(45) Sloop, S. E.; Pugh, J. K.; Wang, S.; Kerr, J. B.; Kinoshita, K. Chemical Reactivity of PF 5 and LiPF6 in Ethylene Carbonate/Dimethyl Carbonate Solutions. *Electrochem. Solid-State Lett.* **2001**, *4*, A42.
(46) Kawamura, T.; Okada, S.; Yamaki, J.-i. Decomposition reaction of LiPF6-based electrolytes for lithium ion cells. *J. Power Sources* **2006**, *156*, 547−554.
(47) Yang, H.; Zhuang, G. V.; Ross, P. N. Thermal stability of LiPF6 salt and Li-ion battery electrolytes containing LiPF6. *J. Power Sources* **2006**, *161*, 573−579.
(48) Wiemers-Meyer, S.; Winter, M.; Nowak, S. Mechanistic insights into lithium ion battery electrolyte degradation − a quantitative NMR study. *Phys. Chem. Chem. Phys.* **2016**, *18*, 26595−26601.
(49) Henschel, J.; Peschel, C.; Klein, S.; Horsthemke, F.; Winter, M.; Nowak, S. Clarification of Decomposition Pathways in a State-of-the-Art Lithium Ion Battery Electrolyte through 13C-Labeling of Electrolyte Components. *Angew. Chem.* **2020**, *132*, 6184−6193.
(50) Botte, G. G.; White, R. E.; Zhang, Z. Thermal stability of LiPF6−EC:EMC electrolyte for lithium ion batteries. *J. Power Sources* **2001**, *97*−*98*, 570−575.
(51) Lux, S. F.; Lucas, I. T.; Pollak, E.; Passerini, S.; Winter, M.; Kostecki, R. The mechanism of HF formation in LiPF6 based organic carbonate electrolytes. *Electrochem. Commun.* **2012**, *14*, 47−50.
(52) Campion, C. L.; Li, W.; Lucht, B. L. Thermal Decomposition of LiPF6-Based Electrolytes for Lithium-Ion Batteries. *J. Electrochem. Soc.* **2005**, *152*, A2327.
(53) Wagner, R.; Korth, M.; Streipert, B.; Kasnatscheew, J.; Gallus, D. R.; Brox, S.; Amereller, M.; Cekic-Laskovic, I.; Winter, M. Impact of Selected LiPF6 Hydrolysis Products on the High Voltage Stability of Lithium-Ion Battery Cells. *ACS Appl. Mater. Interfaces* **2016**, *8*, 30871−30878.
(54) Okamoto, Y. Ab Initio Calculations of Thermal Decomposition Mechanism of LiPF6-Based Electrolytes for Lithium-Ion Batteries. *J. Electrochem. Soc.* **2013**, *160*, A404.

(55) Gebala, A. E.; Jones, M. M. The acid catalyzed hydrolysis of hexafluorophosphate. *J. Inorg. Nucl. Chem.* **1969**, *31*, 771−776.
(56) Rinkel, B. L. D.; Hall, D. S.; Temprano, I.; Grey, C. P. Electrolyte Oxidation Pathways in Lithium-Ion Batteries. *J. Am. Chem. Soc.* **2020**, *142*, 15058−15074.
(57) Liu, M.; Vatamanu, J.; Chen, X.; Xing, L.; Xu, K.; Li, W. Hydrolysis of LiPF $_6$ -Containing Electrolyte at High Voltage. *ACS Energy Lett.* **2021**, *6*, 2096−2102.
(58) Cao, C.; Pollard, T. P.; Borodin, O.; Mars, J. E.; Tsao, Y.; Lukatskaya, M. R.; Kasse, R. M.; Schroeder, M. A.; Xu, K.; Toney, M. F.; Steinrück, H.-G. Toward Unraveling the Origin of Lithium Fluoride in the Solid Electrolyte Interphase. *Chem. Mater.* **2021**, *33*, 7315−7336.
(59) Bi, Y.; Wang, T.; Liu, M.; Du, R.; Yang, W.; Liu, Z.; Peng, Z.; Liu, Y.; Wang, D.; Sun, X. Stability of Li2CO3 in cathode of lithium ion battery and its influence on electrochemical performance. *RSC Adv.* **2016**, *6*, 19233−19237.
(60) Parimalam, B. S.; MacIntosh, A. D.; Kadam, R.; Lucht, B. L. Decomposition Reactions of Anode Solid Electrolyte Interphase (SEI) Components with LiPF6. *J. Phys. Chem. C* **2017**, *121*, 22733−22738.
(61) Leung, K. Two-electron reduction of ethylene carbonate: A quantum chemistry re-examination of mechanisms. *Chem. Phys. Lett.* **2013**, *568*−*569*, 1−8.
(62) An, S. J.; Li, J.; Daniel, C.; Mohanty, D.; Nagpure, S.; Wood, D. L. The state of understanding of the lithium-ion-battery graphite solid electrolyte interphase (SEI) and its relationship to formation cycling. *Carbon* **2016**, *105*, 52−76.
(63) Jayawardana, C.; Rodrigo, N.; Parimalam, B.; Lucht, B. L. Role of Electrolyte Oxidation and Difluorophosphoric Acid Generation in Crossover and Capacity Fade in Lithium Ion Batteries. *ACS Energy Lett.* **2021**, *6*, 3788−3792.
(64) Jayawardana, C.; Rodrigo, N. D.; Rynearson, L.; Lucht, B. L. Difluorophosphoric Acid Generation and Crossover Reactions in LiNixCoyMnzO2 Cathodes Operating at High Voltage. *J. Electrochem. Soc.* **2022**, *169*, 060509.

https://doi.org/10.1021/acsenergylett.2c02351
ACS Energy Lett. 2023, 8, 347−355